Effect of humidity on C_1, C_2 product selectivity for CO_2 reduction in a hybrid gas/liquid electrochemical reactor

Seung-Hoon Lee,[1] Yang Song,[2] Brandon Iglesias,[2] Henry O. Everitt,[3,4,*] and Jie Liu[1,*]

[1]Department of Chemistry, Duke University, Durham, North Carolina 27708, USA

[2]Reactwell, L.L.C. 1441 Canal Street, Lab 301 Box 5b, New Orleans, LA 70112, USA

[3]U.S. Army DEVCOM Army Research Laboratory-South/Rice University, 6100 Main St., Houston, TX 77005 USA

[4]Department of Physics, Duke University, Durham, North Carolina 27708, USA

*Correspondence: heveritt@duke.edu; j.liu@duke.edu

Abstract

Hybrid gas/liquid-fed electrochemical flow reactors are emerging as attractive alternative platforms for the electrolytic conversion of CO_2 into fuels and chemical feedstocks. A current challenge is to understand and optimize catalytic selectivity for producing desired products from these reactors. Using a basic electrolyte to suppress the hydrogen evolution reaction (HER), we explore how the CO_2 reduction reaction is affected by supplying protons on the gas side of the reactor through water vapor added to the flowing CO_2 supply. Although H_2 remains the dominant product under all conditions for constant pH (12.66), supplying dry CO_2 gas selectively produces more C_2 products, including ethanol, while adding protons through water vapor changes selectivity towards C_1 products. Furthermore, by humidifying the CO_2 supply gas, the overall faradaic efficiency of C_1 products increases ~9% while H_2 decreases by ~15% over the tested range. These results suggest that for alkaline environments, selectivity for C_1 or C_2 products is determined by the supply of protons through water vapor in a manner that does not increase the HER.

Keywords: electrochemical CO_2 reduction, hybrid gas/liquid reactor, water vapor management, product selectivity, three-phase interface

TOC GRAPHIC

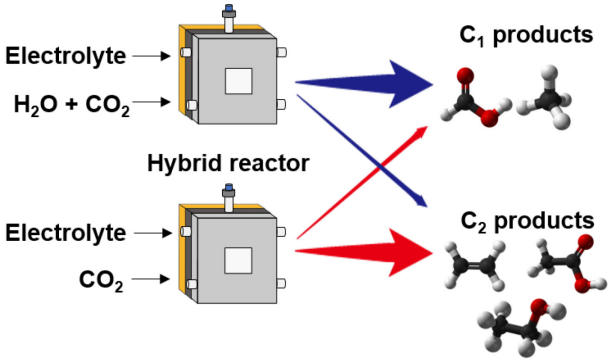
Electrolyte
$H_2O + CO_2$
Hybrid reactor
Electrolyte
CO_2
C_1 products
C_2 products

The release of carbon dioxide (CO_2) from fossil fuels into the atmosphere has triggered environmental concerns about climate change. However, electrochemical conversion of carbon dioxide into fuel and chemical feedstocks offers a way to turn waste into valuable products.[1] While electrochemical CO_2 reduction has been widely studied in conventional liquid-phase "H-cells," mass transport limitations and low CO_2 gas solubility in aqueous electrolytes typically produce low current densities and low product formation rates.[2] To overcome these limitations and obtain high product output, hybrid gas/liquid reactors have been developed.[3,4] These three-chamber, three-electrode hybrid gas/liquid reactors (hereafter referred to as "hybrid reactors") include a gas chamber through which gaseous reactants like CO_2 flow past and through the gas-diffusion electrodes (GDEs) into the electrolyte on the other side. Novel catalysts are deposited onto the GDE so that high concentrations of CO_2 can be maintained in close proximity to the catalyst surface, even at high reaction rates.[3,5] Studies of hybrid reactors have already demonstrated high current densities (>100 mA/cm^2)[6] and high C_2 product selectivity (e.g. faradaic efficiency of $C_2 \sim 85.8\%$),[7] motivating growing interest in hybrid reactors for the CO_2 reduction reaction (CO2RR).[2,5]

Despite these advantages, hybrid reactors exhibit a number of operational difficulties that must be overcome, including electrolyte "flooding:" leakage through the GDE into the gas chamber.[8] Because the reaction occurs at the gas-catalyst-liquid interface, flooding is typically mitigated by applying an appropriate hydrophobic layer to the catalyst that still allows both gaseous diffusion through and some electrolyte diffusion into the porous GDE catalyst.[9] Recent mechanistic studies have provided additional insights about the cause of this flooding,[8] and some novel strategies have proven successful in achieving long-term stability against other factors too, including pH and CO_2 flow rate.[10,11]

Another difficulty is that the thermodynamics and kinetics of the CO2RR within the hybrid reactor are quite different from those found in liquid-phase reactors, exhibiting greater sensitivity to the local environment of the catalyst (esp. pH, CO_2 flow rate, and water concentration at the electrode).[2,4,12,13] In particular, the complex role of water as a source of protons in CO2RR remains unresolved in hybrid reactors.[2,4] Proton generation may be limited in hybrid reactors since the amount of water is small or non-existent in the gas side of hybrid reactors compared to liquid-phase cells where both sides of the cathode and catalysts are thoroughly wetted. Moreover, if the electrode is dry in a hybrid reactor, the electrocatalysts may be inactive due to the limited ionic conducting pathway. Thus, water facilitates ion transport between the anode and cathode, and it supplies protons for CO2RR (and HER).

Many of the desired CO2RR products contain H atoms, and the CO2RR occurs with a sequential proton-coupled electron transfer (PCET) process. Although the initial mechanism for CO_2 activation is still under debate, protons must be available near the active intermediates of CO2RR to promote protonation and produce more hydrocarbons.[12] However, a proton-rich environment, commonly created when using a neutral electrolyte such as 1M $KHCO_3$, can promote the hydrogen evolution reaction (HER) rather than the desired CO2RR.[10] The reduced proton concentration of a high pH electrolyte is known to suppress the competing HER while improving CO2RR by reducing its activation overpotential.[10,14-16] Adjusting the proton population by adjusting pH can increase either HER or CO2RR, and product selectivity towards hydrocarbons or hydrogen will change depending on which process is more favored.[4]

In a hybrid reactor, the opportunity exists to adjust product selectivity, not just between HER and CO2RR but between C_1 and C_2 products, by changing conditions on the gas side while holding electrolyte pH constant. Specifically, protons may be supplied on the gas side through the introduction of water vapor under constant high pH conditions where the proton concentration in the electrolyte is low. Few studies of the effects of humidity on product selectivity have been reported for membrane- or microfluidic-type flow cells, so there is a need to understand how the water vapor content within the gas phase flow cell affects selectivity in order to manage and optimize the performance of CO_2 hybrid gas/liquid flow reactors (both membrane-type and microfluidic-type).[2,4]

Here we report that CO2RR product selectivity in a typical hybrid gas/liquid reactor can be controlled through the gas phase supply of carbon (through CO_2) and protons (through water vapor). Instead of employing widely-used neutral, carbon-containing electrolytes like 1M $KHCO_3$ that are known to act as a carbon and proton source for CO2RR,[17] the carbon-free basic electrolyte 1M KOH was used to (1) manage the supply of carbon from the gas and liquid sides, (2) limit proton availability from the electrolyte, and (3) suppress HER while improving CO2RR.[10,14,15] In our hybrid reactor, reactions occur at the three-phase gas-catalyst-liquid boundary, thereby allowing us to ascertain how the mass transport limitation common in liquid-phase H-cells may be overcome by supplying CO_2 through the gas chamber. Then, by adding water vapor to the supplied CO_2 gas, a good ionic conducting channel is created within the catalyst that supports proton transport, increases the total FE of hydrocarbon products, and improves the stability of the GDE.[18,19] After discussing observations that product selectivity between and within C_1 and C_2 products depend on CO_2 and water vapor content in the gas chamber without increasing the HER, we conclude by investigating how selectivity towards

the specific C_2 product ethanol depends on conditions in the hybrid reactor.

We used a standard three-electrode configuration -- gas chamber, reference cell, and anodic cell -- for the electrochemical CO2RR (Figure 1A).[3] The CO_2 gas, water vapor, and Ar carrier gas flowed through the gas chamber, from which the liquid electrolyte in the reference cell is separated by the GDE catalyst (Figure 1C). The 1M KOH liquid electrolyte flowed into and through the reference and anodic cells separated by an anion exchange membrane. We explored various modifications of the catalyst surface in order to promote water activation and manage protons more effectively,[7,20] always being careful to avoid liquid flooding through the GDE that would limit CO_2 diffusion through the GDE pores.[18]

The GDE cathode used here was composed of randomly oriented carbon fibers covered by a dense nanotextured array of carbon nanospikes (CNSs) approximately 50–80 nm in length (Figure 1B). The CNS were grown on n-type 4-inch Si wafers with As-doping via plasma-enhanced chemical vapor deposition.[21] Each nanospike consisted of layers of puckered carbon, ending in a ~2 nm wide curled tip. A similar catalyst previously showed over 60% CO2RR conversion efficiency toward ethanol when the CNS was coated with copper nanoparticles (NPs).[21] In our work, the carbon fibers were first coated by a hydrophobic layer of polytetrafluoroethylene (PTFE) to prevent electrolyte leakage. Then, an ink containing copper NPs, methanol, nafion, and PTFE particles were spray-cast onto the CNS cathode, producing a copper NP density of ~55 mg/cm^2. The copper NP-coated catalyst faced the electrolyte in the reference cell and was wetted by diffusion of the electrolyte.

The 0.01 g of PTFE particles widely dispersed throughout the catalyst constituted only 10% by weight of the copper by mass (0.1 g), enough to maintain catalyst hydrophobicity while allowing some gas-electrolyte contact. Consequently, the catalyst was wetted without leaking, and the CO2RR occurred at the three-phase boundary (Figure S1).[9,22] Note that we obtained a much higher current density (>100 mA/cm^2) with less PTFE (<10% PTFE in the Cu ink), but that also caused reduced stability, large current fluctuations, and electrolyte leaking within an hour. We added more PTFE to improve stability and product analysis, even though that reduced current density (Figure S2).

We begin with a control experiment by eliminating CO_2 from the gas chamber while bubbling the 1M KOH electrolyte with CO_2 gas in order to ascertain the role of dissolved CO_2 for CO2RR in this reactor. In this “Ar” (0% CO_2) reaction, 10 ml/min of argon gas was flowed through the gas chamber. The pH of the 1M KOH electrolyte remained strongly basic after CO_2 was dissolved, dropping only from 13.91 to 12.66 (see SI). The gas products produced in the

reactor flowed through the gas chamber outlet and were analyzed in real time by a mass spectrometer, while the liquid products passed with the electrolyte through the reference cell outlet and were collected for subsequent NMR analysis (see SI for details). Even with strongly alkaline conditions, hydrogen was the principal product, with a faraday efficiency (FE) that exceeded 75% for all bias potentials (Figure 2A). The only hydrocarbon produced was formic acid, a C_1 product, in tiny amounts with a very low FE (< 1%) over the range of biases tested (-0.8 to -1.3 V). In a second Ar control reaction, only hydrogen was produced, no hydrocarbons, when all carbon-containing species were removed by saturating the electrolyte with Ar instead of CO_2 (Figure S3). These control experiments confirmed that the mass transport limitation of dissolved CO_2 gas within the electrolyte hindered hydrocarbon production.

Next, we explored whether HER could be suppressed and CO2RR improved by controlling the CO_2 gas supply through the gas chamber, since both reactions are competing at the GDE. To explore this question, we replaced Ar with CO_2 flowing at the same rate into the gas chamber (10ml/min, "dry CO_2"). Figures 2B, S5, and S6 show that the products from CO2RR increased dramatically, with C_2 hydrocarbons ethanol, acetic acid, and ethylene in greater abundance than C_1 products methane and formic acid. Although it might be argued that alkaline environments suppress CH_4 formation, we observed a fair amount of CH_4 production (~5-6%) at -0.8V and -0.9V vs. RHE in this alkaline environment, as did another group recently.[7] The current density also increased compared to the Ar condition (Figure 2D), which indicates the CO_2 supply through the gas chamber increased the CO2RR rate. No other carbon-containing compounds were observed, including CO, methanol, ethane, acetylene, and 1-propanol. The HER was suppressed, especially at the lowest bias potentials, but recovered at higher potentials as the CO2RR faltered for each product. Interestingly, the fractional C_2 Faraday efficiency $C_2/(C_1+C_2)$ was approximately 2/3 for all bias potentials (Figure 3A), indicating that total C_2:C_1 hydrocarbon selectivity was a constant 2:1 under these conditions. However, the distribution of C_2 products changed with bias. Of particular interest is the comparative abundance of ethanol (20-30% of all C_2 products, Figure 3B) and its low onset potential (-0.8 V vs RHE) in comparison with the shrinking production of ethylene and acetic acid with increasing bias potential.

It has been shown that an optimal surface concentration of key intermediates, such as *CO, promotes carbon-carbon bonding and enhanced C_2 formation.[23] Our results suggest that the high local CO_2 concentration afforded by CO_2 gas flowing over the GDE catalyst yields greater surface concentrations of these key intermediates, leading to more efficient CO2RR than from

CO_2 dissolved in the electrolyte, especially at low bias. Interestingly, the absence of a gas phase proton source does not hinder this reaction. Indeed, it may be that the dearth of protons allows a longer dwell time for adsorbed carbon intermediates that, in turn, suppresses HER and increases selectivity toward C_2 over C_1 products.

To confirm this hypothesis, we repeated the experiment by humidifying the dry CO_2 supply gas (2.7% water vapor + 97.3% CO_2 = "humidified CO_2"). CO_2 gas was bubbled through a small water bottle for an hour before being allowed to flow into the gas-chamber. We observed that adding water vapor to the gas chamber suppressed hydrogen production even further (Figure 2C), with an averaged FE value ~15% lower than that for dry CO_2 over the same range of bias voltages, and slightly increased total CO2RR products and current density (Figure 2D). Evidently, providing water vapor and CO_2 from the gas side created a more effective pathway for hydrocarbon production than providing either reactant from the liquid side. Indeed, the principal advantage of hybrid gas/liquid reactors is that the facile diffusion of gas phase reactants within the GDE favorably controls product selectivity. Dry CO_2 supplied the gas-facing side of the catalyst with ample adsorbed carbon and a dearth of adsorbed hydrogen so that C_2 products had time to form. Likewise, the addition of water vapor added more adsorbed hydrogen to the gas-facing side of the catalyst so that C_1 products formed more quickly. By contrast, the liquid-facing side of the catalyst was saturated with adsorbed hydrogen and little adsorbed carbon, thus favoring the dominant HER. Although the production rates and current densities were limited by the addition of PTFE to prevent electrolyte flooding, our results indicate an opportunity to tailor reactant diffusivity from both directions within the GDE to improve both selectivity and production rate.

Interestingly, humidified CO_2 gas produced significantly more C_1 products (methane, formic acid) than C_2 products: the C_2 FE fraction $C_2/(C_1+C_2)$ dropped from ~0.68 for dry CO_2 to ~0.39 for humidified CO_2 for all applied biases (Figure 3A). Simply stated, humidifying the CO_2 changed the C_2:C_1 ratio from 2:1 to almost 1:2. These findings indicate that the additional proton supply from water vapor produced more C_1 products than C_2 products or H_2. It has been reported that there are two proton-enabled pathways for CO2RR towards the C_1 product formic acid. One is through *OCHO, which is the first intermediate of CO_2 from a PCET step,[12] and the other is through anionic hydride, yielding *HCOO-.[24] In fact, the theoretical onset potential for formic acid is 0.19 V lower than that for hydrogen production, even though the activation of CO_2 itself is difficult.[25] Methane formation can be also enhanced through protonation.[26] Thus, C_1 production depends sensitively on the availability of protons provided by the water

vapor supply.

As compared to the dry CO_2 condition, humidification also dramatically changed C_2 hydrocarbon selectivity, nearly quenching ethanol and acetic acid production while enhancing ethylene (Figures. 2C, 3B, S6). The onset potential for ethanol increased from -0.8V to -1.3V vs. RHE, while the onset potential remained -0.8 V vs RHE all other products (Figures. 2B, 2C, S4). Recently, enhanced C_2 formation was reported using a hydrogen-assisted C-C coupling mechanism in a fluorine-modified copper catalyst.[7] This catalyst enhanced water dissociation, produced more *H species at the surface, and promoted the overall FE of C_2 products, including ethylene and ethanol. In our measurements, however, humidified CO_2 produced more ethylene but suppressed ethanol and acetic acid formation. It has been reported that these three C_2 products share a common intermediate (*CH_2COH or *COCOH),[27,28] and the increase of FE for one of the C_2 products could result in the suppression of other C_2 products. Our results support this hypothesis, where the enhanced ethylene production is attributed to the suppressed production of ethanol and acetic acid.

Of the C_2 products, only ethanol experienced a change in onset potential from dry to humidified CO_2 gas conditions (Figures. 2, S4). This suggests that ethanol has a different reaction pathway than acetic acid and a higher energy barrier, an observation that conflicts with two recently proposed reaction pathways for CO2RR towards acetic acid and ethanol.[27,29,30] One proposed pathway suggests the disproportionation of acetaldehyde, which can produce acetic acid and ethanol with a 1:1 ratio.[29,30] However, in both our dry and humidified experiments, the overall FE of acetic acid and ethanol deviated significantly from 1:1, especially in the humidified experiments where ethanol was more suppressed than the acetic acid. In the other proposed pathway, acetic acid and ethanol were found to form competitively but with the same onset potential, suggesting a common *CHCO intermediate shared by both.[27] However, in our dry CO_2 experiments, acetic acid and ethanol decreased together rather than competing, and in our humidified experiments, the onset potential for ethanol was significantly higher that of the acetic acid (Figure S4). Considering all this, we find that these three C_2 products may share a common intermediate (ex. *CH_2COH or *COCOH), but ethanol appears to have an additional intermediate or reaction pathway with a higher energy barrier than acetic acid and ethylene.

In summary, product selectivity for CO2RR in a hybrid gas/liquid electrocatalytic reactor with a GDE catalyst is sensitively determined by the concentration of CO_2 gas and water vapor in the gas chamber without increasing the HER. By using a basic 1M KOH electrolyte with

dissolved CO_2 and constant pH to ascertain the role of these gas phase reactants, we find that C_2 products prefer dry CO_2 conditions, C_1 products prefer humidified CO_2 conditions, and virtually no hydrocarbons are produced when Ar replaces CO_2 in the gas chamber. Although the reaction is dominated by HER, we find that (1) dissolved CO_2 contributes little to the observed products, (2) the additional proton supply from water vapor produces more C_1 products than the C_2 products without producing more hydrogen, and (3) each C_2 product has a different reaction pathway. The addition of protons through water vapor not only enhances C_1 products but changes the selectivity among C_2 products. Notably, we observed a significantly reduced onset potential and greater selectivity for ethanol production under dry CO_2 conditions as compared humidified CO_2 conditions, suggesting that the pathway for ethanol production differs from that for ethylene and acetic acid when protons are provided through the gas chamber. Our work reveals that selectivity control is possible in hybrid reactors by controlling the gas concentration at constant pH: supplying gas phase CO_2 overcomes the mass transport diffusion limitation of dissolved CO_2 and water vapor controls the proton supply and selects for or against reaction pathways under proton-depleted alkaline conditions.

ASSOCIATED CONTENT

Supporting information

The following files are available free of charge at

Polytetrafluoroethylene (PTFE) treatment on CNS cathode; Preparation of Catalyst; Electrochemical measurements; pH measurement after CO_2 bubbling, and calculation of carbonate; NMR measurements; Gas signal measurement in mass spectrometer

Author information

Corresponding Authors

Henry O. Everitt – *U.S. Army DEVCOM Army Research Laboratory-South/Rice University, 6100 Main St., Houston Texas 77005, USA,* and *Department of Physics, Duke University, Durham, North Carolina 27708, USA;* Email: heveritt@duke.edu

Jie Liu – *Department of Chemistry, Duke University, Durham, North Carolina 27708, USA;* Email: j.liu@duke.edu

Authors

Seung-Hoon Lee – *Department of Chemistry, Duke University, Durham, North Carolina 27708, USA*

Yang Song – *Reactwell, L.L.C. 1441 Canal Street, Lab 301 Box 5b, New Orleans, LA 70112, USA*

Brandon Iglesias – *Reactwell, L.L.C. 1441 Canal Street, Lab 301 Box 5b, New Orleans, LA 70112, USA*

Author Contributions

S.-H.L built the experimental set-up, synthesized, chaterized the material, and performed all of the experiments. B.I and Y.S built the hybrid gas/liquid reactor and synthesized the CNS sample. All of the authors analyzed data, and contributed to writing the manuscript. All authors have given approval to the final version of the manuscript.

Notes

The authors declare no competing financial interest

Acknowledgments

This research was supported in part by the National Science Foundation (grant number CHE-1954838), the U.S. Air Force small business technology transfer research program (contract FA8649-22-P-0099), and the Center for Nanophase Materials Sciences (CNMS), which is a US Department of Energy, Office of Science User Facility at Oak Ridge National Laboratory. The authors also acknowledge support by the Duke University Shared Materials Instrumentation Facility (SMIF), a member of the North Carolina Research Triangle Nanotechnology Network (RTNN), which is supported by the National Science Foundation (Grant ECCS-1542015) as part of the National Nanotechnology Coordinated Infrastructure (NNCI). S-HL was partially supported by an appointment to the Department of Defense (DOD) Research Participation Program administered by the Oak Ridge Institute for Science and Education (ORISE) through an interagency agreement between the U.S. Department of Energy (DOE) and the DOD. ORISE is managed by ORAU under DOE contract number DE-SC0014664. All opinions expressed in this paper are the author's and do not necessarily reflect the policies and views of DOD, DOE, or ORAU/ORISE.

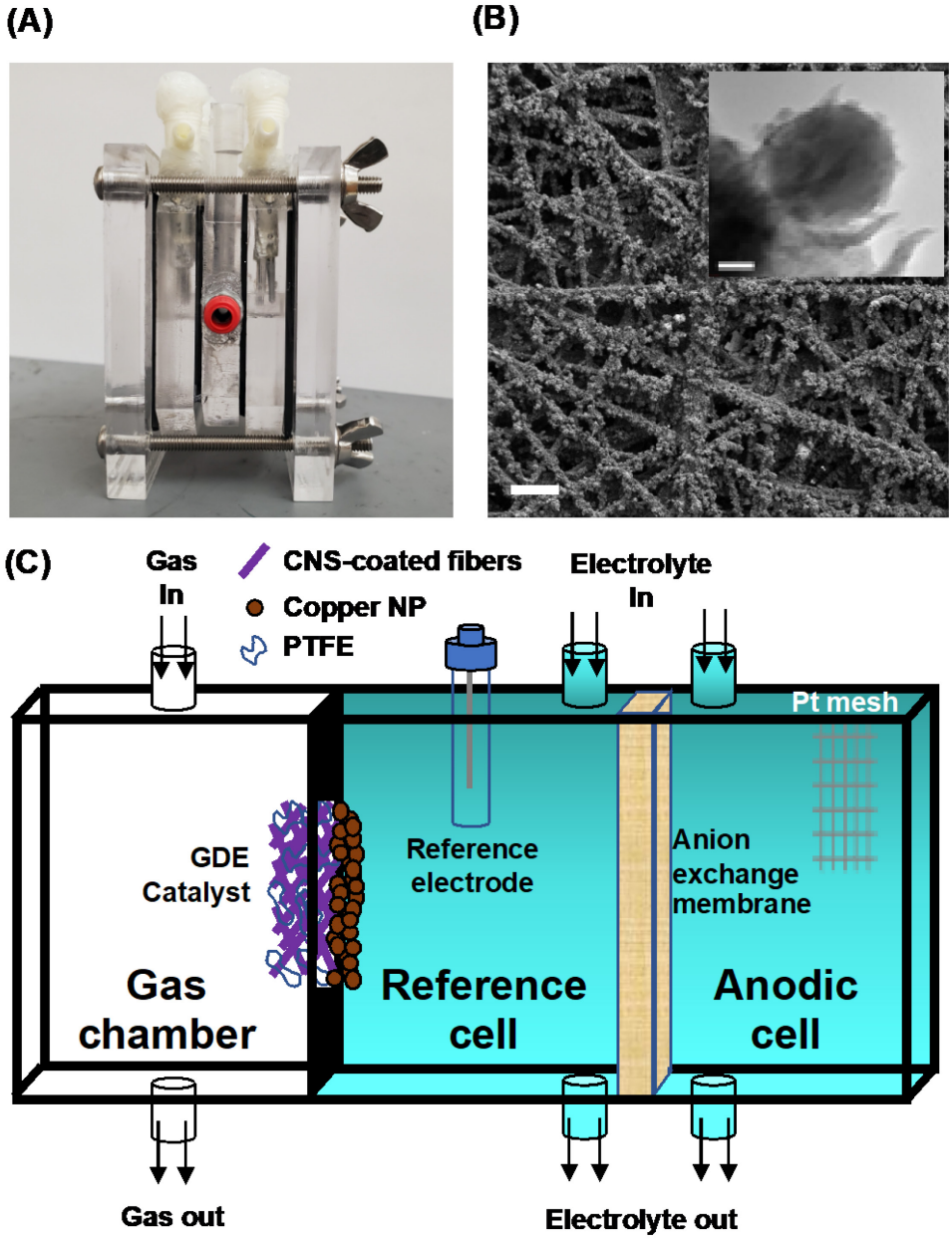

Figure 1. (A) Optical image of the hybrid gas/liquid reactor composed of three cells: gas chamber (left), reference cell (center), and anodic cell (right). (B) A scanning electron microscope image of the CNS-coated GDE catalyst, showing the copper NP-coated carbon fibers from which the carbon nanospikes extend (60 µm scale bar). The non-conductive PTFE is not observable in this SEM image. The inset shows the copper NP-CNS catalyst (10 nm scale bar). (C) Illustration of the three-cell hybrid gas/liquid reactor, with the GDE separating the gas and reference cells and the anion exchange membrane separating the reference and anodic cells.

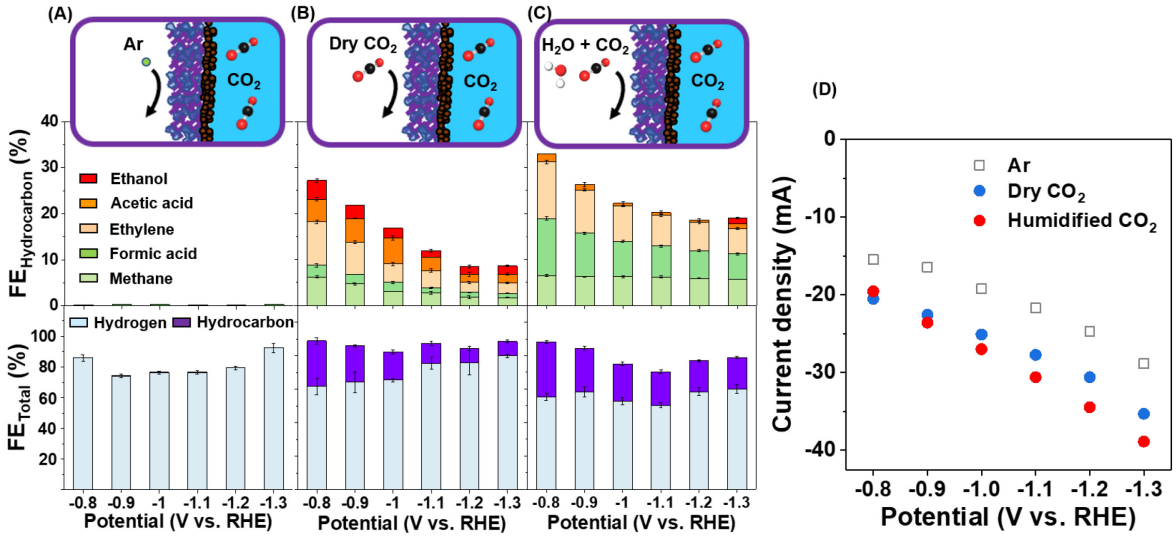

Figure 2. (A-C) Illustration of the three gas conditions (A) Ar (0% CO_2), (B) dry CO_2, and (C) humidified CO_2 explored in the gas chamber of the hybrid reactor. The top plots show the measured FE of just the hydrocarbon products, while the bottom plots show the total FE for all products under these conditions. (D) Measured total current density under these three gas conditions.

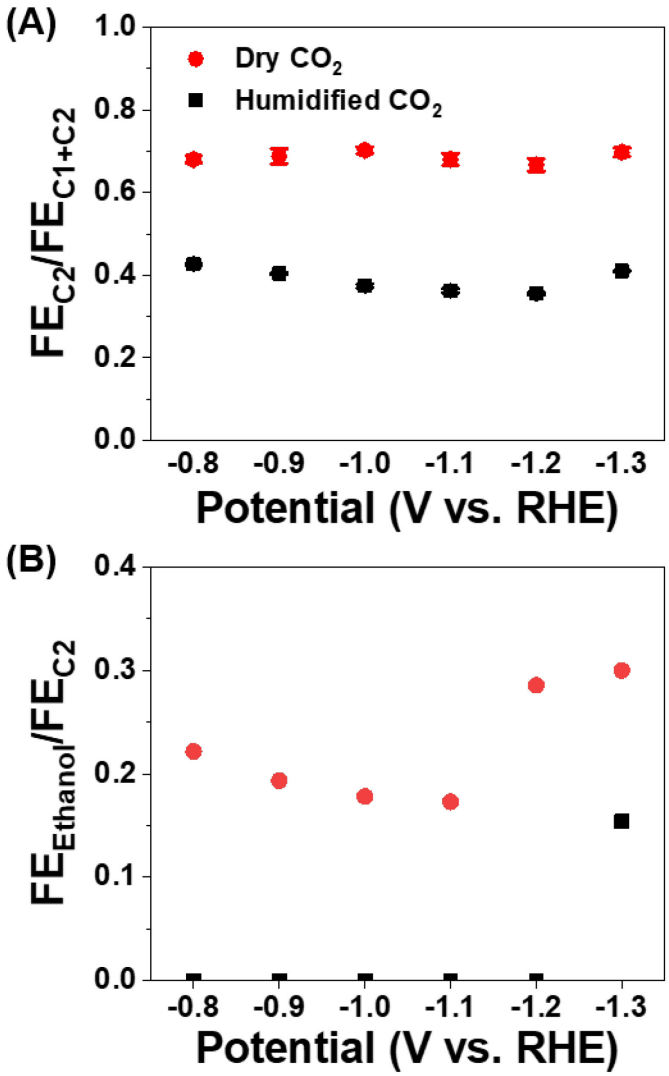

Figure 3. (A) C_2 / hydrocarbon FE fraction ($FE_{C2/C1+C2}$) and (B) ethanol / C_2 FE fraction ($FE_{Ethanol}/FE_{C2}$) at different applied potentials under the dry CO_2 (red) and humidified CO_2 (black) conditions.

Reference

(1) Luna, P. D.; Hahn, C.; Higgins, D.; Jaffer, S. A.; Jaramillo, T. F.; Sargent, E. H. What would it take for renewably powered electrosynthesis to displace petrochemical processes? *Science* **2019**, *364*, eaav3506.
(2) Weekes, D. M.; Salvatore, D. A.; Reyes, A.; Huang, A.; Berlinguette, C. P. Electrolytic CO_2 Reduction in a Flow Cell. *Acc. Chem. Res.* **2018**, *51*, 910-918.
(3) Liu, K.; Smith, W. A.; Burdyny, T. Introductory Guide to Assembling and Operating Gas Diffusion Electrodes for Electrochemical CO_2 Reduction. *ACS Energy Lett.* **2019**, *4*, 639-643.
(4) Lees, E. W.; Mowbray, B. A. W.; Parlane, F. G. L.; Berlinguette, C. P. Gas diffusion electrodes and membranes for CO_2 reduction electrolysers. *Nat. Rev. Mater.* **2022**, *7*, 55-64.
(5) Nguyen, T. N.; Dinh, C.-T. Gas diffusion electrode design for electrochemical carbon dioxide reduction. *Chem. Soc. Rev.* **2020**, *49*, 7488-7504.
(6) Arquer, F. P. G. d.; Dinh, C.-T.; Ozden, A.; Wicks, J.; McCallum, C.; Kirmani, A. R.; Nam, D.-H.; Gabardo, C.; Seifitokaldani, A.; Wang, X.; et al. CO_2 electrolysis to multicarbon products at activities greater than 1 Acm^{-2}. *Science* **2020**, *367*, 661-666.
(7) Ma, W.; Xie, S.; Liu, T.; Fan, Q.; Ye, J.; Sun, F.; Jiang, Z.; Zhang, Q.; Cheng, J.; Wang, Y. Electrocatalytic reduction of CO_2 to ethylene and ethanol through hydrogen-assisted C–C coupling over fluorine-modified copper. *Nat. Catal.* **2020**, *3*, 478-487.
(8) Yang, K.; Kas, R.; Smith, W. A.; Burdyny, T. Role of the Carbon-Based Gas Diffusion Layer on Flooding in a Gas Diffusion Electrode Cell for Electrochemical CO_2 Reduction. *ACS Energy Lett.* **2021**, *6*, 33-40.
(9) Burdyny, T.; Smith, W. A. CO_2 reduction on gas-diffusion electrodes and why catalytic performance must be assessed at commercially-relevant conditions. *Energy Environ. Sci.* **2019**, *12*, 1442-1453.
(10) Dinh, C.-T.; García de Arquer, F. P.; Sinton, D.; Sargent, E. H. High Rate, Selective, and Stable Electroreduction of CO_2 to CO in Basic and Neutral Media. *ACS Energy Lett.* **2018**, *3*, 2835-2840.
(11) Dinh, C.-T.; Burdyny, T.; Kibria, M. G.; Seifitokaldani, A.; Gabardo, C. M.; Arquer, F. P. G. d.; Kiani, A.; Edwards, J. P.; Luna, P. D.; Bushuyev, O. S.; et al. CO_2 electroreduction to ethylene via hydroxide-mediated copper catalysis at an abrupt interface. *Science* **2018**, *360*, 783-787.
(12) Birdja, Y. Y.; Pérez-Gallent, E.; Figueiredo, M. C.; Göttle, A. J.; Calle-Vallejo, F.; Koper, M. T. M. Advances and challenges in understanding the electrocatalytic conversion of carbon dioxide to fuels. *Nat. Energy* **2019**, *4*, 732-745.
(13) Gao, D.; Arán-Ais, R. M.; Jeon, H. S.; Roldan Cuenya, B. Rational catalyst and electrolyte design for CO_2 electroreduction towards multicarbon products. *Nat. Catal.* **2019**, *2*, 198-210.
(14) Verma, S.; Hamasaki, Y.; Kim, C.; Huang, W.; Lu, S.; Jhong, H.-R. M.; Gewirth, A. A.; Fujigaya, T.; Nakashima, N.; Kenis, P. J. A. Insights into the Low Overpotential Electroreduction of CO_2 to CO on a Supported Gold Catalyst in an Alkaline Flow Electrolyzer. *ACS Energy Lett.* **2018**, *3*, 193-198.
(15) Nitopi, S.; Bertheussen, E.; Scott, S. B.; Liu, X.; Engstfeld, A. K.; Horch, S.; Seger, B.; Stephens, I. E. L.; Chan, K.; Hahn, C.; et al. Progress and Perspectives of Electrochemical CO_2 Reduction on Copper in Aqueous Electrolyte. *Chem. Rev.* **2019**, *119*, 7610-7672.
(16) Kastlunger, G.; Wang, L.; Govindarajan, N.; Heenen, H. H.; Ringe, S.; Jaramillo, T.; Hahn, C.; Chan, K. Using pH Dependence to Understand Mechanisms in Electrochemical CO Reduction. *ACS Catal.* **2022**, *12*, 4344-4357.
(17) Li, T.; Yang, C.; Luo, J.-L.; Zheng, G. Electrolyte Driven Highly Selective CO_2 Electroreduction at Low Overpotentials. *ACS Catal.* **2019**, *9*, 10440-10447.

(18) Reyes, A.; Jansonius, R. P.; Mowbray, B. A. W.; Cao, Y.; Wheeler, D. G.; Chau, J.; Dvorak, D. J.; Berlinguette, C. P. Managing Hydration at the Cathode Enables Efficient CO_2 Electrolysis at Commercially Relevant Current Densities. *ACS Energy Lett.* **2020**, *5*, 1612-1618.
(19) Li, Y. C.; Zhou, D.; Yan, Z.; Gonçalves, R. H.; Salvatore, D. A.; Berlinguette, C. P.; Mallouk, T. E. Electrolysis of CO_2 to Syngas in Bipolar Membrane-Based Electrochemical Cells. *ACS Energy Lett.* **2016**, *1*, 1149-1153.
(20) Ma, W.; Xie, S.; Zhang, X.-G.; Sun, F.; Kang, J.; Jiang, Z.; Zhang, Q.; Wu, D.-Y.; Wang, Y. Promoting electrocatalytic CO_2 reduction to formate via sulfur-boosting water activation on indium surfaces. *Nat. Commun.* **2019**, *10*, 892.
(21) Song, Y.; Peng, R.; Hensley, D. K.; Bonnesen, P. V.; Liang, L.; Wu, Z.; Meyer III, H. M.; Chi, M.; Ma, C.; Sumpter, B. G.; et al. High-Selectivity Electrochemical Conversion of CO_2 to Ethanol using a Copper Nanoparticle/N-Doped Graphene Electrode. *ChemistrySelect* **2016**, *1*, 6055-6061.
(22) Xing, Z.; Hu, L.; Ripatti, D. S.; Hu, X.; Feng, X. Enhancing carbon dioxide gas-diffusion electrolysis by creating a hydrophobic catalyst microenvironment. *Nat. Commun.* **2021**, *12*, 136.
(23) Tan, Y. C.; Lee, K. B.; Song, H.; Oh, J. Modulating Local CO_2 Concentration as a General Strategy for Enhancing C−C Coupling in CO_2 Electroreduction. *Joule* **2020**, *4*, 1104-1120.
(24) Solis, B. H.; Maher, A. G.; Dogutan, D. K.; Nocera, D. G.; Hammes-Schiffer, S. Nickel phlorin intermediate formed by proton-coupled electron transfer in hydrogen evolution mechanism. *Proc. Natl. Acad. Sci.* **2016**, *113*, 485-492.
(25) Fan, L.; Xia, C.; Yang, F.; Wang, J.; Wang, H.; Lu, Y. Strategies in catalysts and electrolyzer design for electrochemical CO_2 reduction toward C_{2+} products. *Sci. Adv.* **2020**, *6*, eaay3111.
(26) Wang, X.; Xu, A.; Li, F.; Hung, S.-F.; Nam, D.-H.; Gabardo, C. M.; Wang, Z.; Xu, Y.; Ozden, A.; Rasouli, A. S.; et al. Efficient Methane Electrosynthesis Enabled by Tuning Local CO_2 Availability. *J. Am. Chem. Soc.* **2020**, *142*, 3525-3531.
(27) Luc, W.; Fu, X.; Shi, J.; Lv, J.-J.; Jouny, M.; Ko, B. H.; Xu, Y.; Tu, Q.; Hu, X.; Wu, J.; et al. Two-dimensional copper nanosheets for electrochemical reduction of carbon monoxide to acetate. *Nat. Catal.* **2019**, *2*, 423-430.
(28) Hanselman, S.; Koper, M. T. M.; Calle-Vallejo, F. Computational Comparison of Late Transition Metal (100) Surfaces for the Electrocatalytic Reduction of CO to C2 Species. *ACS Energy Lett.* **2018**, *3*, 1062-1067.
(29) Nagai, Y.; Morooka, S.; Matubayasi, N.; Nakahara, M. Mechanisms and Kinetics of Acetaldehyde Reaction in Supercritical Water: Noncatalytic Disproportionation, Condensation, and Decarbonylation. *J. Phys. Chem. A* **2004**, *108*, 11635-11643.
(30) Birdja, Y. Y.; Koper, M. T. M. The Importance of Cannizzaro-Type Reactions during Electrocatalytic Reduction of Carbon Dioxide. *J. Am. Chem. Soc.* **2017**, *139*, 2030-2034.